Uncertainty assessment and comparison of different dose algorithms used to evaluate a two element LiF:Mg,Ti TL personal dosemeter

H. Stadtmann*, C. Hranitzky,

Austrian Research Centers GmbH – ARC, 2444 Seibersdorf, Austria.

Abstract. This paper presents the results of an uncertainty assessment and comparison study of different dose algorithms used for evaluating our routine two element TL whole body dosemeter. Due to the photon energy response of the two different filtered LiF:Mg,Ti detector elements the application of dose algorithms is necessary to assess the relevant photon doses over the rated energy range with an acceptable energy response. Three dose algorithms are designed to calculate the dose for the different dose equivalent quantities, i.e. personal dose equivalent $H_p(10)$ and $H_p(0.07)$ and photon dose equivalent H_x used for personal monitoring before introducing personal dose equivalent. Based on experimental results both for free in air calibration as well as calibration on the ISO water slab phantom (type test data) a detailed uncertainty analysis war performed by means of Monte Carlo simulation techniques**.** The uncertainty contribution of the individual detector element signals was taken into special consideration.

KEYWORDS: TLD; Personal dosemeter, dose algorithm; dose quantity; measurement uncertainty

1 Introduction/Scope

The scope of this paper is to present the results of a comparison of an uncertainty assessment using different dose algorithms for evaluating a two element thermoluminescent (TL) whole body dosemeter. Three dose algorithms were designed to calculate the dose in terms of three different dose quantities H_x, H_p (10) and H_p (0.07) (respectively, the photon dose equivalent, and the personal dose equivalents at 10 and 0.07 mm depth). Both, the resulting response functions as well as the calculated uncertainties of the different dose algorithms were compared.

2 Dosemeter design

The beta-photon personal dosemeter investigated in this work consists of a commercial two element TL-card and an in-house designed dosemeter badge (figure 1) used in our routine Dosimetry Service Seibersdorf. The TL card contains two LiF:Mg,Ti (TLD-100) detector elements. One TL detector is only covered with a thin Mylar foil, whereas the other TL detector is below a 2 mm aluminium/Noryl filter combination.

This dosemeter was originally designed for the measurement of the dose quantity photon dose equivalent H_x based on a free-in-air calibration. However it was already foreseen during the design phase to use the same dosemeter for the measurement of the operational quantities $H_p(10)$ and additionally $H_p(0.07)$. These quantities recommended by ICRU are based however on the calibration of the dosemeter on the ISO slab phantom applying dose conversion coefficients h_{pK} given in ICRU 57 [1] and ISO 4037-3 [2]. The main differences between H_x, $H_p(10)$ and $H_p(0.07)$ are their different energy and angular responses related to the basic field quantities such as air kerma free in air. Details on these quantities are given in table 1. The differences can partially be considered by the application of appropriate mathematical algorithms for each dose quantity combining the two readings from each of the detector elements.

* Presenting author, E-mail: hannes.stadtmann@arcs.ac.at

Table 1: Summary of different dose quantities used for the calibration of personal whole body dosemeters.

Symbol	Quantity	Relation to basic field quantity	SI Unit	Calibration of dosemeter
K_a	Air kerma	= basic field quantity	Gy	Free in air
X	Exposure	= basic field quantity	$C.kg^{-1}$	Free in air
H_x	Photon dose equivalent	$H_x = 0.01$ [Sv/R]· X	Sv	Free in air
$H_p(10)$	Personal dose equivalent	$H_p(10) = h_{pK}(10, E, \alpha) K_a$	Sv	On water slab phantom
$H_p(0.07)$	Personal dose equivalent	$H_p(0.07) = h_{pK}(0.07, E, \alpha) K_a$	Sv	On Water slab phantom

Figure 1: Whole body dosemeter of the routine Dosimetry Service Seibersdorf.

3 Dose algorithms and energy response

Due to the energy response of the LiF:Mg,Ti detectors a dose algorithm is necessary to assess the relevant dose over the rated energy range with an acceptable energy dependence as defined in recent international standards for passive dosemeters (IEC 61066 [3] and IEC 62387-1 [4]). All three discussed dose algorithms are designed to measure doses for different dose quantities. A summary of these algorithms and the recommended energy ranges are given in table 2. The first algorithm is used to evaluate the dose quantity *photon dose equivalent* H_x. This quantity was the legal quantity in Austria and Germany for the last decades and is directly related to the quantity *exposure* X (table 1). The other two algorithms are designed for reading out the whole dosemeter in terms of the operational dose quantities personal dose equivalents, H_p (10) and H_p (0.07). These dose calculation algorithms mathematically combine the signal of the two detector elements TL_i (i=window or filter), corrected for individual detector efficiency and reader sensitivity.

In figure 2 experimental determined energy response curves normalised to photon radiation of ^{137}Cs (S-Cs) of both detector elements (TL_w and TL_f) are given for the three different dose quantities. These measurements were carried out at the calibration laboratory Seibersdorf applying narrow spectrum photon radiation qualities (N-Series) according to ISO-4037-1 [5]. Only irradiations from the reference direction, perpendicular to the card are considered in figure 2. Both the definition of the applied dose quantity as well as the fact that measurements were performed free in air (for H_x) or on the water slab phantom (for $H_p(10)$ and $H_p(0.07)$) result in pronounced differences of the energy responses of the two detector elements especially in the lower energy region (E < 30 keV).

Table 2: Summary of 3 dose algorithms discussed in this paper . TL_i (i=window and filter), readings of the two card detector elements corrected for individual detector efficiency, reader sensitivity and zero reading, N Calibration factor of the readout system, a_{10} and $a_{0.07}$ weighting parameters according to the dose model equation (2).

Algorithm	Quantity	Math. Algorithm	Energy range	Comment
#1	H_x	$H_x = N\ TL_f$ for $TL_w/TL_f > 0.7$ $H_x = 0.8\ N\ TL_w$ for $TL_w/TL_f < 0.7$	15 – 1300 keV	"if" algorithm with 2 linear branches Reference photon energy: 662 keV
#2	$H_p(10)$	$H_p(10) = N\ [a_{10}TL_w + (a_{10}\text{-}1)\ TL_f]$ $a_{10} = 0.71$	20 – 1300 keV	Linear Algorithm Reference photon energy: 662 keV
#3	$H_p(0.07)$	$H_p(0.07) = N\ [a_{0.07}TLw + (a_{0.07}\text{-}1)\ TL_f]$ $a_{0.07} = 0.09$	20 – 1300 keV	Linear Algorithm Reference photon energy: 100 keV

Figure 2 a, b, c: Relative energy response for photon dose equivalent (H_x) for a free in air calibration and relative energy response for personal dose equivalent $H_p(10)$ and $H_p(0.07)$ for a calibration on the water slab phantom. Both the values for the detector elements (TL_w, TL_f) as well as the dose results after application of the dose algorithms are presented.

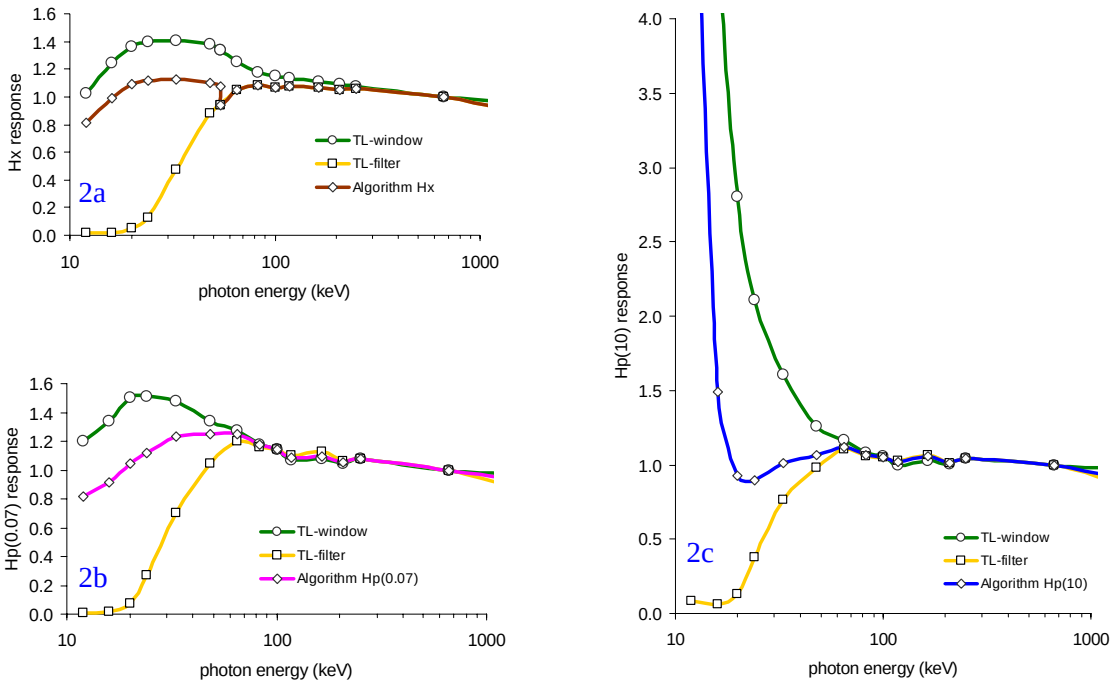

4 Comparison of different dose algorithms

Figure 2 demonstrates the possibility to calculate the different doses in the appropriate dose quantity by applying a mathematical algorithm to the individual detector readings. Since a personal dosemeter is always worn on the body of a person the recommended dosemeter calibration procedure for H_x - free in air - is not relevant for the dosemeter reading. On the basis of the measured results given in figure 2 it is possible to calculate in how far a free in air calibrated dosemeter (applying algorithm #1 for the dose quantity H_x) can estimate the two operational quantities $H_p(10)$ and $H_p(0.07)$.

Figure 3 shows the ratios $H_x/H_p(10)$ and $H_x/H_p(0.07)$. It can be seen that a dosemeter indication in terms of H_x is also a good estimate for $H_p(10)$ for energies above 40 keV. For the estimation of $H_p(0.07)$ the useful energy range is even extended to 15 keV.

It is important to consider that the results given in figure 3 are properties of the personal dosemeter itself. It is not possible to calculate these data just by converting the different dose quantities by the application of the dose conversion factors given in ICRU57 [1] or ISO 4037-3 [2]. The specific sensitivity of the dosemeter for backscattered radiation from the phantom (or the person wearing the dosemeter) influences the response functions of the dosemeter.

Figure 3: dose ratio of the reading of a free in air calibrated dosemeter reading in H_x and both the true value for the personal dose equivalent $H_p(10)$ and $H_p(0.07)$.

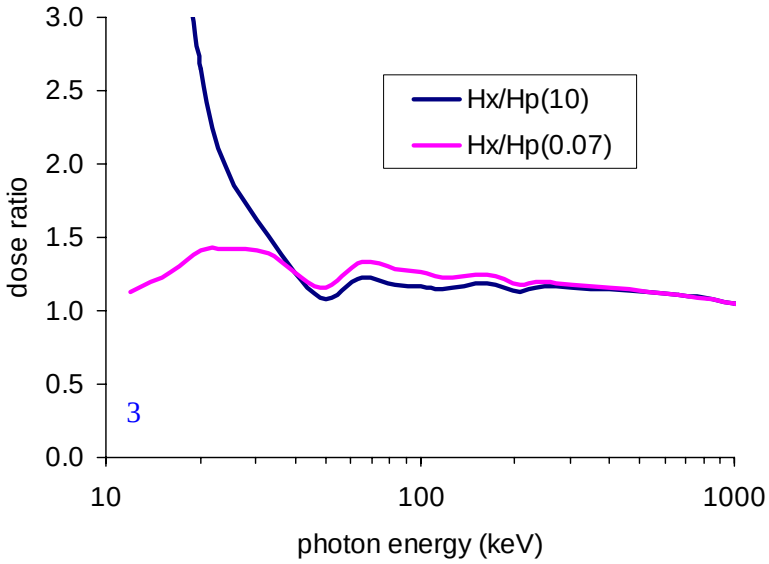

5 Considering the angular response

So far discussed data consider irradiations from the reference direction. Figure 4 shows the combined energy and angular response of the dosemeter for the dose quantities $H_p(10)$ and $H_p(0.07)$. By considering the angular response the extreme limits of the response function increase over the rated energy range. These values however are still well within the range (0.69 – 1.67) recommended by (IEC61066 [3] and IEC62387-1 [4]).

Figure 4 a, b: The combined energy and angular response of the personal dosemeter for both dose quantities $H_p(10)$ and $H_p(0.07)$. The considered angular range covers a cone of ±60° from reference direction as recommended by IEC 62387-1. The angular response is marked as a black bar in the diagram. The extreme values of the response function over the whole energy range (20keV – 1250 keV) are marked in addition in red.

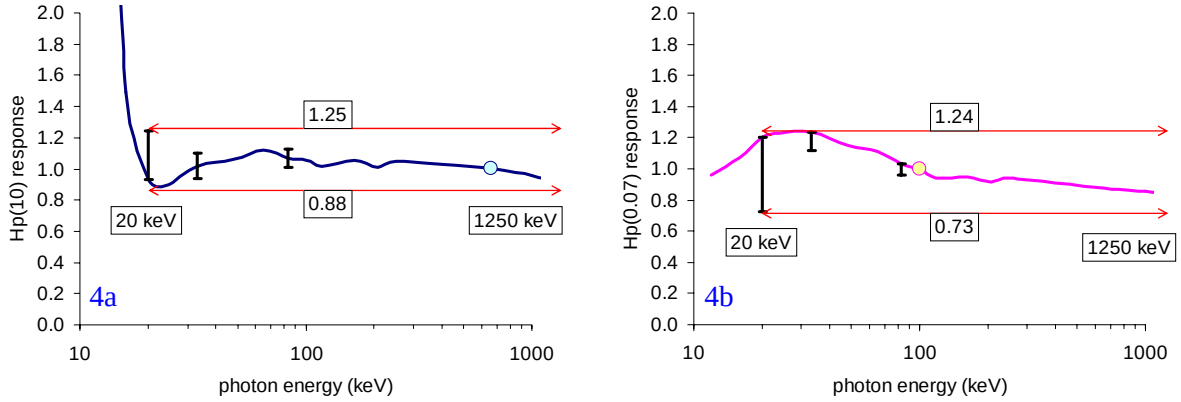

6 Uncertainty assessment

The combined energy and angular response of the dosemeter is the main contribution to the uncertainty budget of the dosemeter in conditions where the irradiation conditions are not well defined or unknown. In the following section two different approaches to assess the uncertainty are described and the results are compared.

6.1 Analytical uncertainty assessment

In the technical report IEC 62461 [6] - which serves as a practical introduction to the GUM [7] with special emphasis on measurements in radiation protection - examples of the analytical uncertainty assessment for passive dosimetric systems are given. In this document different distribution functions for the input quantities are discussed and also recommended. According to this technical report an uncertainty analysis for the dosemeter output in terms of $H_p(10)$ and $H_p(0.07)$ was performed. The following dose **model function** considering the applied dose algorithms was used:

$$H_p = N_0 \cdot k_{E,\varphi} \cdot k_{env} \cdot \left(a \cdot \left(TL_w + TL_{w0} - TL_0\right) + (a-1) \cdot \left(TL_f + TL_{f0} - TL_0\right)\right) \qquad \textbf{(1)}$$

Output quantity:

H_p	measuring quantity personal dose equivalent $H_p(10)$ or $H_p(0.07)$

Input Quantities:

N_0	reference **calibration factor**
$k_{E,\varphi}$	**correction factor** for photon energy and angle of incidence
k_{env}	**correction factor** for environmental conditions (fading etc.)
TL_i	detector signal (readout) of the TL element (i = w or f)
TL_{i0}	zero readout of the TL element (i = w or f) including also deviation due to EMC

Parameters:

a	dose algorithm parameter a_{10} or $a_{0.07}$ (see table 2)
TL_0	mean zero readout of the TL elements

Table 3: Summary of the **uncertainty budget** for different dose quantities $H_p(10)$ and $H_p(0.07)$ and different dose values (1 mSv and 0.1 mSv).

input quantity	output quantity	distribution	standard uncertainty	uncertainty contribution to the output quantity (mSv)			
				$H_p(10)$= 1mSv	$H_p(0.07)$= 1mSv	$H_p(10)$= 0.1mSv	$H_p(0.07)$= 0.1mSv
N	$H_p(d)$	triangle	$0.1/6^{1/2}$	0.0408	0.0408	0.0041	0.0041
k_{env}	$H_p(d)$	gaussian (3σ)	0.15/3	0.0500	0.0500	0.0500	0.0500
$k_{E,\varphi}$	$H_p(10)$	gaussian (3σ)	0.2/3	0.0667	-	0.0067	-
$k_{E,\varphi}$	$H_p(0.07)$	gaussian (3σ)	0.37/3	-	0.1233	-	0.0123
TL_w	$H_p(d)$	gaussian	0.05	0.0155	0.0492	0.0015	0.0049
TL_f	$H_p(d)$	gaussian	0.05	0.0387	0.0049	0.0039	0.0005
TL_{w0}	$H_p(d)$	gaussian	0.015 mSv	0.0046	0.0148	0.0031	0.0098
TL_{f0}	$H_p(d)$	gaussian	0.015 mSv	0.0116	0.0015	0.0077	0.0010
combined standard uncertainty u_c				0.1025	0.1485	0.0161	0.0209
expanded standard uncertainty U (k=2)				**0.2050**	**0.2970**	**0.0322**	**0.0419**
relative expanded standard uncertainty U_{rel} (k=2)				**20.5%**	**29.7%**	**32.2%**	**41.9%**

The calculation results in an expanded uncertainty between 20% and 42% depending on both, the dose quantity - $H_p(0.07)$ shows higher uncertainties - and the dose value itself. This analytical approach assumes that all input and output quantities are described by symmetric uncertainty distributions. This is the reason why in recent standards (IEC 61066 [3] and IEC 62387-1 [4]) the performance requirements for the combined energy and angular **response values $R_{E,\varphi}$** are asymmetric (-29%, +67%) to receive symmetric borderers (±40%) for the corresponding **correction factor $K_{E,\varphi}$** = 1/ $R_{E,\varphi}$.

6.2 Numerical uncertainty assessment by Monte Carlo simulation

To overcome the restriction of symmetric uncertainty distribution of the input quantities a general numerical uncertainty assessment by means of Monte Carlo (MC) simulations was performed. For this purpose the professional programme package @RISK was used. @RISK performs risk and uncertainty analysis using any spreadsheet (Microsoft Excel) calculation as model function. A wide range of different probability density functions (PDFs) can be assigned to the input quantities (spreadsheet cell). The resulting PDF of the output quantity can be simulated and analysed by a wide range of statistical methods.

The measured energy and angular response of the detector signals were used to calculate (by interpolation) the complete $TL_i(E, \varphi)$ matrix as a function of photon energy (E) and direction of radiation incidence (φ). The model function for simulating the **dosemeter response** is:

$$R_{Hp} = \frac{1}{N \cdot k_{env} \cdot H_p} \cdot \left(a \cdot R_w(E,\varphi) \cdot \left(TL_w + TL_{w0} - TL_0\right) + (a-1) \cdot R_f(E,\varphi) \cdot \left(TL_f + TL_{f0} - TL_0\right)\right) \quad \textbf{(2)}$$

With:

$R_{Hp}(E,\varphi)$ dosemeter response in terms of $H_p(10)$ or $H_p(0.07)$
$R_i(E,\varphi)$ combined energy and angular response for the individual detector element (i = w or f) in terms of $H_p(10)$ or $H_p(0.07)$

Other symbols see equation (1)

Table 4: Summary of the **PDFs** of the input quantities for the Monte Carlo simulation.

input quantity	Distribution	parameters	remark
N	Triangle	±0.1	
k_{env}	gaussian (3σ)	±0.15 (=3σ)	
E	hyperbolic	20 keV – 1250 keV	Results in a uniform distribution on the logarithmic energy axis
φ	uniform	±60°	
TL_w, TL_f	gaussian	σ = 0.05	
TL_{w0} , TL_{f0}	lognormal	Mean: 0.015 mSv σ = 0.015 mSv	Only positive values possible

In table 4 the applied probability density distributions and parameter values of the input quantities according equation (2) are presented. For the input quantities N, k_{env}, TL_w, TL_f, the similar distributions described in table 3 were used. For the zero reading TL_{w0} and TL_{f0} a more realistic asymmetric lognormal distribution was introduced.

In figure 5 and 6 both the MC-simulated frequency distributions for the simulated $H_p(10)$ and $H_p(0.07)$ response values as well as some statistical parameters for the distributions are given. The $H_p(10)$ distribution is symmetrical gaussian shaped. The mean value of all response values 0.998 is close to 1. The $H_p(0.07)$ distribution however shows a strong deviation from a normal distribution. This distribution seems to be a super composition of two components. The mean value of all response values 0.963 is still close to 1. In figure 6 the resulting distribution for the ratio of the reading of a free in air calibrated dosemeter (H_x) and both the personal dose equivalent $H_p(10)$ and $H_p(0.07)$ is given. Equivalent to the data given in figure 3 an over response for $H_p(10)$ up to a factor of 3 of this H_x dosemeter appears. On the other hand the dose quantity $H_p(0.07)$ can be estimated by this H_x dosemeter sufficiently.

Figure 5 a, b: MC-simulated frequency distribution of the dosemeter response for both dose quantities $H_p(10)$ and $H_p(0.07)$ for a constant dose value of $H_p(10)$ = 1 mSv

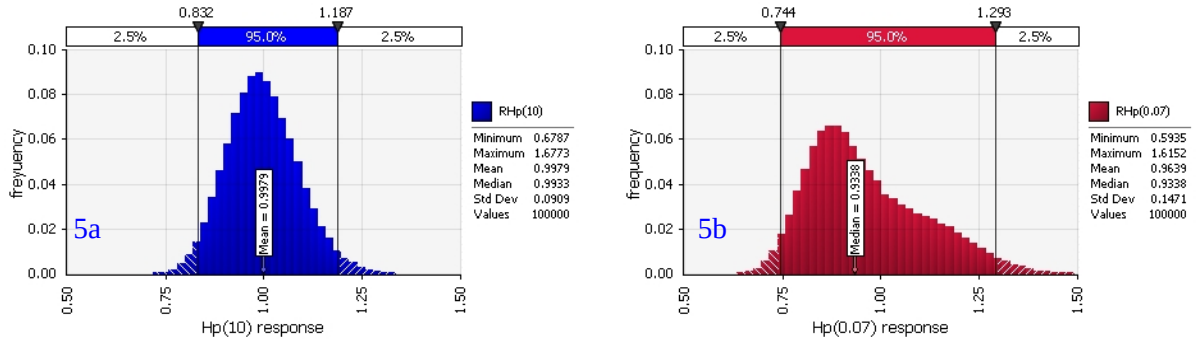

Figure 6 a, b: MC-simulated frequency distribution of the dose ratio of the reading of a free in air calibrated dosemeter (H_x) and both the personal dose equivalent $H_p(10)$ and $H_p(0.07)$.

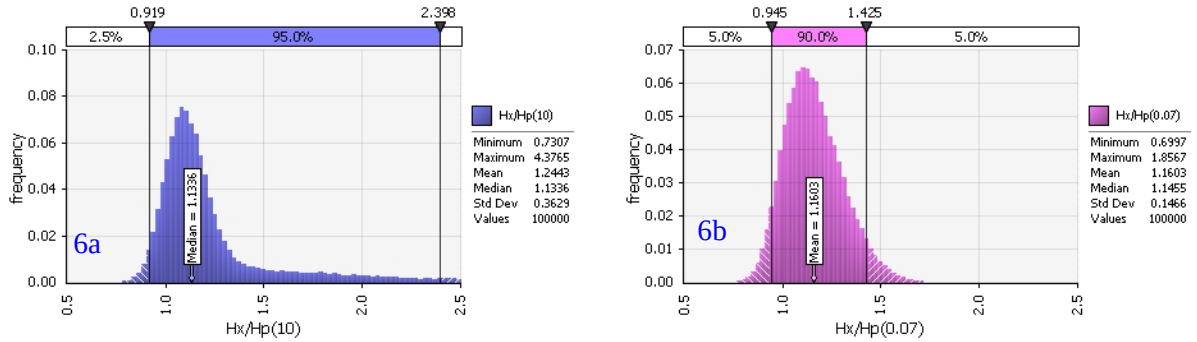

Figure 7 a, b: MC-simulated frequency distribution of the ratio of the two detector readings (TL-window and TL-filter). In figure b (right) the simulated cumulative frequency distribution is compared to the distribution of real measured individual dose values.

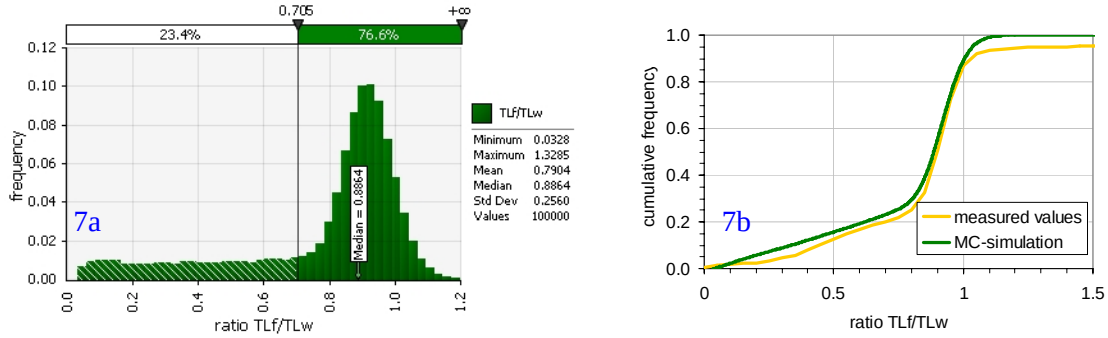

In figure 7 the resulting distribution of the ratio of the two detector readings (TL-window and TL-filter) is given. About one quarter of all simulated values show a ratio below 0.7. The ratio exceeds in 11% of all readings unity (this is caused by the uncertainty attributed to the single detector reading). This is in good agreement with measured values. As a proof the cumulative probability function of these values is compared in figure 7b with measured ones, i.e. dosemeter readings of occupationally radiation exposed workers [8]. The shape of both functions is in good agreement.

7 Summary and discussion

This work proved that the described two element dosemeter can be evaluated in terms of 3 different dose quantities applying different algorithms with a satisfactory energy response. The energy range covers 20 keV to 1250 keV. When the angular response is considered in addition, the combined energy and angular response fulfils the requirements of IEC 61066 [3] and IEC 62387-1 [4]

Two independent methods (analytical approach and Monte Carlo simulations) for estimating the uncertainties of the dose calculations (by the different algorithms) were performed. Both approaches show similar results although some PDFs of the input quantities as well as some PDFs of the resulting output quantities where not Gaussian shaped. The comparison of distribution parameters received by the two different uncertainty assessments are summarised in table 5.

Uncertainty assessment by Monte Carlo simulation requires the possibility to simulate the detector signals for different photon energies and angles of incidents. To simulate the radiation fields a hyperbolic energy distribution and a uniform angle distribution was used. Although this approach seems to be heuristic, the resulting distribution of the ratio of the two detector signals shows a good agreement with experimental data (figure 7b).

Table 5: Comparison of distribution parameters received by different uncertainty assessments. $R_{low}(95\%)$ and $R_{high}(95\%)$ are the lower and upper limit of the response range were 95% of all values are located.

	$H_p(10)$=1mSv		$H_p(0.07)$=1mSv	
	analytical approach	MC-simulation	analytical approach	MC-simulation
$R_{low}(95\%)$	0.796	0.832	0.703	0.744
$R_{high}(95\%)$	1.205	1.187	1.298	1.293

The free in air calibrated dosemeter for H_x that was used for the last decades however can estimate $H_p(10)$ for energies exceeding 40 keV. At lower energies an over response (up to the factor 2.4) occurred. The dose quantity $H_p(0.07)$ however can be estimated by the H_x calibrated dosemeter satisfactory over the whole energy range.

8 Conclusion

MC simulation is an appropriate tool to perform uncertainty calculations. The possibility to assign arbitrary PDFs to the input quantities, as well as define complex model function (not even necessarily differentiable) allows the simulation of irradiation conditions close to reality. In this paper the energy and angular range of the simulated values cover the whole rated range (low level consideration), to estimate the uncertainty without detailed information about the irradiation conditions. In the next step it is foreseen – for specific dosimeter readouts only - to consider all additional available information (e.g. the energy distribution characterising different workplace radiation fields) to improve the measured dose and reduce the uncertainty of the result (high level consideration). For this purpose MC simulation is considered to be the ideal tool.

References

[1] ICRU. Report 57, Conversion Coefficients for use in Radiological Protection against External Radiation, [1998)

[2] ISO Report 4037-3, X and Gamma Reference Radiation for Calibrating Dosemeters and Doserate Meters and for Determining their Response as a Function of Photon Energy- Part 3: Calibration Area and Personal Dosemeters as a Function of Energy and Angle of Incidence (1999)

[3] IEC 61066, Radiation protection instrumentation—Thermoluminescence Dosimetry systems for personal and environmental monitoring. Edition 2 IEC (2006).

[4] IEC 62387-1. Radiation protection instrumentation — passive integrating dosimetry systems for environmental and personal monitoring — art 1: general characteristics and performance requirements. IEC (2007).

[5] ISO Report 4037-1: X and gamma reference radiation for calibrating dosemeters and doserate meters and for determining their response as a function of photon energy -- Part 1: Radiation characteristics and production methods (1996)

[6] IEC 62461 TR. Radiation protection instrumentation— determination of uncertainty in measurement. IEC (2006).

[7] ISO,. Guide to the expression of uncertainty in measurement. Supported by BIPM, IEC, IFCC, ISO, IUPAC, IUPAP and OIML (Geneva: ISO) (1995)

[8] H. Stadtmann; C. Hranitzky, Comparison of different dose algorithms used to evaluate a two element LiF:Mg,Ti TL personal dosemeter, Radiation Measurements Volume 43 Issues 2-6, , pp 571-575 (2008)